

Article

Effect of Blending of Shellac, Carbonyl Iron Powder, and Carbonyl Iron Powder/Carbon Nanotube Microcapsules on the Properties of Coatings

Ye Zhu ^{1,2}, Wenbo Li ^{1,2}, Yongxin Xia ^{1,2}, Jingyi Hang ^{1,2}, Xiaoxing Yan ^{1,2,*} and Jun Li ^{1,2}

¹ Co-Innovation Center of Efficient Processing and Utilization of Forest Resources, Nanjing Forestry University, Nanjing 210037, China; zhuye@njfu.edu.cn (Y.Z.); liwenbo@njfu.edu.cn (W.L.); xiayongxin@njfu.edu.cn (Y.X.); hangjingyi@njfu.edu.cn (J.H.); lijun0099@njfu.edu.cn (J.L.)

² College of Furnishings and Industrial Design, Nanjing Forestry University, Nanjing 210037, China

* Correspondence: yanxiaoxing@njfu.edu.cn

Abstract: Nine sets of orthogonal experimental samples were prepared by examining four factors: shellac microcapsules, carbonyl iron powder (CIP) microcapsules, CIP/ carbon nanotube (CNT) microcapsules, and primer coating thickness. By testing the morphology and performance of the coating and using the fracture elongation of the coating as an orthogonal experimental analysis, the maximum factor affecting the fracture elongation of shellac, CIP, and CIP/CNT microcapsule coatings was determined. The first two factors that had a significant impact on the fracture elongation of the coating were the content of CIP/CNT microcapsules and shellac microcapsules. In order to further optimize the coating performance, important factor experiments were conducted, using the content of CIP/CNT microcapsules and shellac microcapsules as variables. It was found that the coating had the best performance when the content of CIP/CNT microcapsules was 7.0% and the content of shellac microcapsules was 4.0%. The optical properties of coatings with added shellac, CIP, and CIP/CNT microcapsules were tested, and the color difference and glossiness of the coatings showed little change. The mechanical properties of coatings with added shellac, CIP, and CIP/CNT microcapsules were tested. The blending of the three types of microcapsules enhanced the toughness of the coating to a certain extent, and suppressed the generation of micro-cracks, demonstrating a good self-healing effect. The electromagnetic-absorption performance of coatings with added shellac, CIP, and CIP/CNT microcapsules was tested. The blending of shellac, CIP, and CIP/CNT microcapsules exhibited two effective bands of electromagnetic absorption and a good absorption performance at a relatively wide frequency range. The combination of shellac, CIP, and CIP/CNT microcapsules endows the fiberboard surface with self-healing and electromagnetic-absorption functions, while maintaining the original performance of the water-based coating. The results can be used for application of surface coatings on wooden materials with dual functions of self-healing and electromagnetic absorption.

Keywords: blending of microcapsules; fracture elongation; toughness; self-healing



Citation: Zhu, Y.; Li, W.; Xia, Y.; Hang, J.; Yan, X.; Li, J. Effect of Blending of Shellac, Carbonyl Iron Powder, and Carbonyl Iron Powder/Carbon Nanotube Microcapsules on the Properties of Coatings. *Coatings* **2024**, *14*, 75. <https://doi.org/10.3390/coatings14010075>

Received: 22 November 2023

Revised: 21 December 2023

Accepted: 30 December 2023

Published: 5 January 2024



Copyright: © 2024 by the authors. Licensee MDPI, Basel, Switzerland. This article is an open access article distributed under the terms and conditions of the Creative Commons Attribution (CC BY) license (<https://creativecommons.org/licenses/by/4.0/>).

1. Introduction

Wood is the only renewable, recyclable, and naturally degradable green material among the four major materials in the world [1,2]. It is widely used in industries such as furniture manufacturing, building structures, and papermaking [3–6]. However, wood is prone to cracking, due to the dry shrinkage and wet expansion characteristics [7]. In addition, wood contains lignin, cellulose, and hemicellulose, which are easily degraded into glucose, water, and carbon dioxide, leading to wood decay and deterioration, and reducing service life [8–10]. A commonly used method to extend the service life of wooden products is to apply coatings on the surface of wood for protection [11,12]. The water-based coatings use water as the dispersion medium, which is easier to obtain than an

organic solvent, greatly saving resources [13]. The water-based coatings have two major advantages: environmental friendliness and safety. With the further implementation of environmental protection policies, the water-based wood coatings have gradually replaced traditional solvent-based wood coatings, and have certain applications in the furniture industry [14,15].

Microcapsules refer to a type of micro-container or packaging with a polymer wall-shell. It has the semi-permeable or sealing properties of small particles. The content wrapped in microcapsules is called a core material, and that wrapped outside the core material is called a wall material. The research on microcapsule technology began in the 1930s, when the Atlantic Coast Fisheries Company of the United States proposed a method for preparing microcapsules of fish liver oil. In 1954, Green from the NCR Corporation in the United States successfully prepared oil-containing gelatin microcapsules, using the complex coagulation method. The microcapsules were used to prepare carbon-free copy paper [16–19]. Microcapsules have the ability to change the state of materials, protect sensitive components, enhance stability, control core-material release, reduce bad odors, and isolate components. Therefore, the microcapsule technology has been widely applied in food, medicine, textiles, coatings, agriculture, cosmetics industry, and other fields. The core-to-wall ratio has a significant impact on the drug loading and particle size of the prepared microcapsules. When the core-to-wall ratio is high, the repair rate of microcapsules is higher. When the core-to-wall ratio is low, the mechanical properties of microcapsules are better. When the core material is a volatile substance, the core-to-wall ratio should be reduced, and when the viscosity of the wall material is high, the core-to-wall ratio should be increased.

Self-healing materials can be divided into two types: intrinsic and extrinsic. The extrinsic self-healing materials based on microcapsules have a high repair efficiency, which has good application prospects [20]. In 2001, White et al. [21] first prepared self-healing microcapsules using dicyclopentadiene (DCPD) and urea formaldehyde resin. Then the Grubbs catalyst and self-healing microcapsules were added to an epoxy resin matrix, achieving a good self-healing effect. Kessler et al. [22] prepared the microcapsules with DCPD as the core material, using the in situ polymerization method. They discussed the relationship between a particle size of microcapsules and a self-healing efficiency. The self-healing microcapsules required catalysts, and the catalysts also required a microencapsulation. However, the introduction of catalysts has a certain impact on the matrix. Therefore, Suryanarayana et al. [23] prepared the microcapsules using a linseed oil as the core material without catalysis, and a polyurea formaldehyde as the wall material. The thickness of the wall material was 200 nm, and the coverage rate was around 80%.

Smart homes not only bring convenience to people, but also bring more electromagnetic radiation hazards. Long-term electromagnetic radiation poses an undeniable threat to the natural environment, human health, and information security. Electromagnetic-absorption materials are prepared in microcapsules and applied to water-based coatings, which can prevent the harm of electromagnetic radiation to the human body and broaden the application range of water-based coatings on fiberboard surfaces. Among various traditional electromagnetic-absorption materials [24,25], magnetic metal materials have a high saturation magnetization and high magnetic permeability. This can achieve better impedance matching with air, thereby reducing coating thickness and increasing electromagnetic-absorption bandwidth. They are ideal choices for developing high-performance electromagnetic-absorption materials [26]. As a typical magnetic metal powder, carbonyl iron powder (CIP) has been widely used as an absorbent, due to the high magnetic permeability, high saturation magnetization, high Curie temperature, excellent absorption performance, and wide electromagnetic-absorption frequency band [27–31]. The coatings with a shell-like structure on CIP magnetic cores [32] have advantages such as a low density, high specific surface area, and large pores. This structure can effectively reduce electromagnetic-absorption density, adjust dielectric constant, and improve impedance matching [33], demonstrating an excellent electromagnetic-absorption

ability [34]. Carbon nanotubes (CNTs) have the characteristics of a wide electromagnetic-absorption frequency, large specific surface area, light weight, and good electromagnetic shielding performance. Through a material composite method, CIP/CNT composite materials can achieve a coordinated effect of multiple scattering, conductive loss, magnetic loss, and interface polarization loss. Then, absorbing materials with thin thickness, wide frequency band, high absorption strength, and good stability can be prepared. However, due to the poor compatibility of CIP and CNTs with the water-based coatings, the overall toughness of the coating is poor, and prone to cracking. Microcapsule modification of CIP and CNTs can decrease these defects, and it is possible to further extend the electromagnetic-loss ability of electromagnetic-absorption microcapsules. In practical applications, dielectric-loss electromagnetic-absorption materials are often combined with magnetic-loss electromagnetic-absorption materials to improve the electromagnetic-absorption performance. The combination of CIP and CNTs can increase the effective absorption-frequency band of electromagnetic-absorption materials, meet the requirements of “wide, thin, strong, and light” electromagnetic-absorption materials, and improve the impedance matching of materials. Shellac microcapsules have good self-healing performance. The combination of three types of microcapsules can enhance the self-healing performance of the coating, while further enhancing the electromagnetic-absorption performance.

The shellac, CIP, and CIP/CNT microcapsules were blended to prepare the coatings. By conducting orthogonal experiments with four factors and three levels, the morphology and properties of the coating were analyzed to determine the maximum and secondary factors affecting the fracture elongation of coatings with added shellac, CIP, and CIP/CNT microcapsules. Then, important factor experiments were conducted. The optimal ratio through experiments such as optics, mechanics, self-healing, and cold resistance was explored to ensure the optimal coating performance, while improving the electromagnetic-absorption performance of coatings with added shellac, CIP, and CIP/CNT microcapsules. To avoid defects such as cracking and bubbling, which may occur in water-based coatings during long-term use, a microencapsulated shellac coating technology was used to modify the water-based coatings, endowing them with self-healing performance. The combination of shellac, CIP, and CIP/CNT microcapsules endows the fiberboard surface with self-healing and electromagnetic-absorption functions, while maintaining the original performance of water-based coating.

2. Materials and Methods

2.1. Materials

Table 1 shows the list of raw materials. A 100 mm × 100 mm × 5 mm-sized fiberboard was selected. The main components of the primer and topcoat (Akzo Nobel Coatings Co., Ltd., Shanghai, China) are water-based acrylic copolymer dispersions.

2.2. Preparation and Optimization of Coating with Blending of Shellac, CIP, and CIP/CNT Microcapsules

2.2.1. Preparation of Shellac Microcapsules

According to Reference [35], the wall material was melamine resin, and the core material was 12.5% yellow shellac solution and rosin solution. The shellac microcapsules with the mass ratio of core material to wall material (0.8:1) were prepared.

2.2.2. Preparation of CIP Microcapsules

According to Reference [36], the wall material was melamine resin, and the core material was CIP. The CIP microcapsules with the mass ratio of core material to wall material (0.65:1) were prepared.

Table 1. List of raw materials.

| Material | Molecular Mass | CAS | Manufacturer |
|------------------|----------------|-------------|--|
| Melamine | 126.12 | 108-78-1 | Tianjin Kemio Chemical Reagent Co., Ltd., Tianjin, China |
| Formaldehyde | 30.03 | 50-00-0 | Guangzhou Yijubao Animal Pharmaceutical Co., Ltd., Guangzhou, China |
| Shellac solution | - | - | Henan Detai Chemical Products Co., Ltd., Zhengzhou, China |
| Rosin solution | - | - | Guangzhou Debao Technology Co., Ltd., Guangzhou, China |
| 75.0% ethanol | 46.07 | 64-17-5 | Shandong Ruikang Pharmaceutical Group Co., Ltd., Yantai, China |
| CIP | 55.845 | 13463-40-6 | Qinghe County Science and Technology Metallurgical Materials Co., Ltd., Xingtai, China |
| CNTs | 12.01 | 308068-56-6 | Suqian Nakaite New Material Technology Co., Ltd., Suqian, China |
| Fiberboard | - | - | Nanjing Hongyang Decoration City Plate Store, Nanjing, China |
| Red ink | - | - | M&G Chenguang Stationery Co., Ltd., Shanghai, China |
| Detergent | - | - | Liby Science and Technology, Guangzhou, China |

2.2.3. Preparation of CIP/CNT Microcapsules

According to Reference [37], the wall material was melamine resin, and the core material was the mixture of CNTs and CIP. The CIP/CNT microcapsules with the mass ratio of core material to wall material (0.50:1) were prepared.

Based on the research [35–37], under the above core-to-wall ratio, the self-healing performance of shellac microcapsules was good, and the electromagnetic-absorption performance of CIP and CIP/CNT microcapsules was good.

2.2.4. Preparation of Coatings with Blending of Shellac, CIP, and CIP/CNT Microcapsules

The preliminary tests have been conducted on the microcapsules of shellac, CIP, and CIP/CNTs, respectively [35–37]. This paper aims to control the key factors based on the previous stage, in order to achieve good mechanical and electromagnetic-absorption performance while ensuring a good repair rate, thereby achieving the best coating performance. The nine sets of orthogonal experimental samples were prepared by examining four factors: shellac microcapsules, CIP microcapsules, CIP/CNT microcapsules, and primer thickness (Table 2). Table 3 shows an arrangement of orthogonal experiments. Table 4 shows the material dosage for preparing coating with mixed microcapsules. Three types of microcapsules were added in different amounts to the water-based primer. The mass of primer was controlled to 4.00 g. They were stirred thoroughly and evenly. The required thickness of primer coating was applied on the glass slide, using an SZQ four-sided coating preparation device (Guangdong Canrd New Energy Technology Co., Ltd., Guangdong, China). The SZQ four-sided coating preparation device has four different thicknesses on the surface. When preparing the coating, a certain amount of coating was placed on a glass slide; both ends of the coating preparation device were held by hand, and gently translated. The application method of the topcoat was the same as that of the primer. No microcapsules were added to the topcoat, and the wet coating thickness was controlled to 60 μm . The coating was peeled off slowly, with a blade, after curing at room temperature for 1 day, and the fracture elongation and repair rate were tested. With the fracture elongation of the coating as the result of the orthogonal experiment, the maximum influencing factor and the second influencing factor were selected. Six different levels under the maximum influencing factor were designed, and experiments at two different levels under the second largest influencing factor were conducted, to explore the optimal mixing ratio of the three microcapsules. The experimental process is shown in Figure 1.

Table 2. Four factors and three levels for preparation of coatings with blending of shellac, CIP, and CIP/CNT microcapsules.

| Content of Shellac Microcapsules (%) | Content of CIP Microcapsules (%) | Content of CIP/CNT Microcapsules (%) | Primer Thickness (μm) |
|--------------------------------------|----------------------------------|--------------------------------------|------------------------------------|
| 1.0 | 1.0 | 1.0 | 10 |
| 2.0 | 3.0 | 3.0 | 20 |
| 3.0 | 5.0 | 5.0 | 25 |

Table 3. Orthogonal experimental schedule for mixed microcapsules.

| Sample (#) | Content of Shellac Microcapsules (%) | Content of CIP Microcapsules (%) | Content of CIP/CNT Microcapsules (%) | Primer Thickness (μm) |
|------------|--------------------------------------|----------------------------------|--------------------------------------|------------------------------------|
| 1 | 1.0 | 1.0 | 1.0 | 10 |
| 2 | 1.0 | 3.0 | 3.0 | 20 |
| 3 | 1.0 | 5.0 | 5.0 | 25 |
| 4 | 2.0 | 1.0 | 3.0 | 25 |
| 5 | 2.0 | 3.0 | 5.0 | 10 |
| 6 | 2.0 | 5.0 | 1.0 | 20 |
| 7 | 3.0 | 1.0 | 5.0 | 20 |
| 8 | 3.0 | 3.0 | 1.0 | 25 |
| 9 | 3.0 | 5.0 | 3.0 | 10 |

Table 4. Material dosage for preparing coating with mixed microcapsules.

| Sample (#) | Shellac Microcapsules (g) | CIP Microcapsules (g) | CIP/CNT Microcapsules (g) | Water-Based Primer (g) |
|------------|---------------------------|-----------------------|---------------------------|------------------------|
| 1 | 0.04 | 0.04 | 0.04 | 3.88 |
| 2 | 0.04 | 0.12 | 0.12 | 3.72 |
| 3 | 0.04 | 0.20 | 0.20 | 3.56 |
| 4 | 0.08 | 0.04 | 0.12 | 3.76 |
| 5 | 0.08 | 0.12 | 0.20 | 3.60 |
| 6 | 0.08 | 0.20 | 0.04 | 3.68 |
| 7 | 0.12 | 0.04 | 0.20 | 3.64 |
| 8 | 0.12 | 0.12 | 0.04 | 3.72 |
| 9 | 0.12 | 0.20 | 0.12 | 3.56 |

According to the orthogonal experimental results, the content of CIP microcapsules was controlled to 1.0%, and the thickness of the primer was controlled to 10 μm . The important factor experiments were conducted with the content of CIP/CNT microcapsules and shellac microcapsules as variables. The higher the content of CIP/CNT microcapsules, the greater the fracture elongation of the coating. However, a high powder content can lead to an uneven dispersion in the coating. Therefore, the content of CIP/CNT microcapsules was set at 4.0%, 5.0%, 6.0%, 7.0%, 8.0%, and 9.0%, respectively. The content of shellac microcapsules was the second largest influencing factor. The fracture elongation of the coating was directly proportional to the content of shellac microcapsules. But excessive content of shellac microcapsules can make them aggregate in the coating, so the content of shellac microcapsules cannot be too high. The content of shellac microcapsules was set at 2.0% and 4.0%, respectively, for important-factor experimental analysis. Table 5 shows the important-factor experiment schedule, and Table 6 shows the material amount for the important-factor experiment.

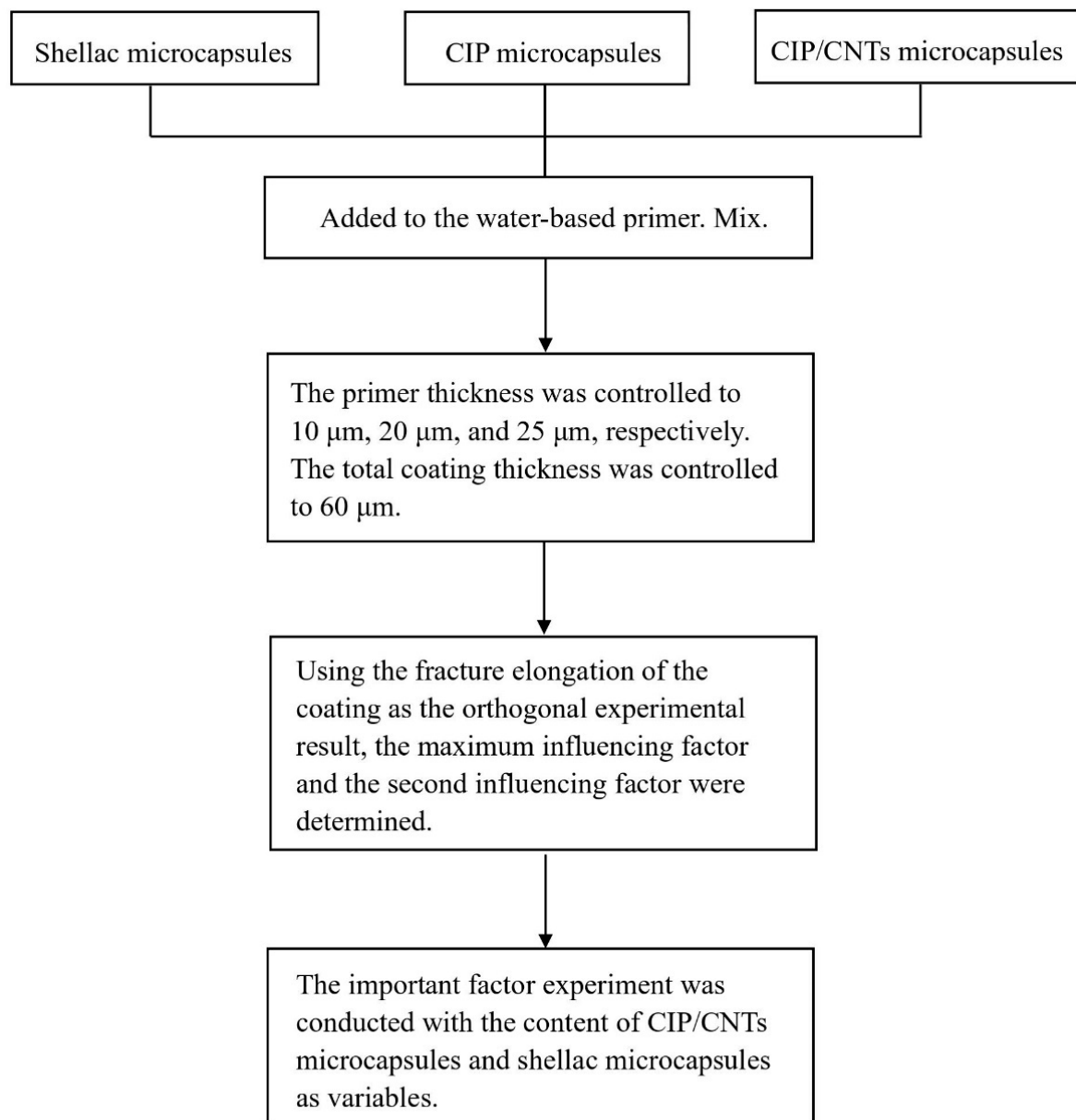


Figure 1. A schematic drawing.

Table 5. Important-factor experiment schedule.

| Content of Shellac Microcapsules (%) | Content of CIP/CNT Microcapsules (%) | Content of CIP Microcapsules (%) | Primer Thickness (μm) |
|--------------------------------------|--------------------------------------|----------------------------------|------------------------------------|
| 2.0 | 4.0 | 1.0 | 10 |
| | 5.0 | 1.0 | 10 |
| | 6.0 | 1.0 | 10 |
| | 7.0 | 1.0 | 10 |
| | 8.0 | 1.0 | 10 |
| | 9.0 | 1.0 | 10 |
| 4.0 | 4.0 | 1.0 | 10 |
| | 5.0 | 1.0 | 10 |
| | 6.0 | 1.0 | 10 |
| | 7.0 | 1.0 | 10 |
| | 8.0 | 1.0 | 10 |
| | 9.0 | 1.0 | 10 |

Table 6. Material amount for important-factor experiment.

| Shellac Microcapsules (g) | CIP/CNT Microcapsules (g) | CIP Microcapsules (g) | Primer (g) |
|---------------------------|---------------------------|-----------------------|------------|
| 0.08 | 0.16 | 0.04 | 3.72 |
| | 0.20 | 0.04 | 3.68 |
| | 0.24 | 0.04 | 3.64 |
| | 0.28 | 0.04 | 3.60 |
| | 0.32 | 0.04 | 3.56 |
| | 0.36 | 0.04 | 3.52 |
| 0.16 | 0.16 | 0.04 | 3.64 |
| | 0.20 | 0.04a | 3.60 |
| | 0.24 | 0.04 | 3.56 |
| | 0.28 | 0.04 | 3.52 |
| | 0.32 | 0.04 | 3.48 |
| | 0.36 | 0.04 | 3.44 |

2.3. Testing and Characterization

2.3.1. Microscopic Characterization

When the pressure was below 3 Kpa, the sample was observed using a scanning electron microscope. An optical microscope was adjusted to the appropriate magnification to observe a small amount of sample.

2.3.2. Chemical Composition

When detecting the chemical composition of the sample, a Vertex 80V Fourier-transform infrared spectrometer (FTIR, Shenyang Jiasco Trading Co., Ltd., Shenyang, China) was used.

2.3.3. Optical Properties

According to GB/T 11186.3-1989 [38], the instrument used when testing the color difference of the coating was a Ci64 color difference meter (Aiselei (Shanghai) Color Technology Co., Ltd., Shanghai, China). The color difference ΔE between two positions was calculated according to the CIELAB color difference formula, as shown in Formula (1), where $\Delta L = L_1 - L_2$, $\Delta a = a_1 - a_2$, and $\Delta b = b_1 - b_2$.

$$\Delta E = \sqrt{(\Delta L)^2 + (\Delta a)^2 + (\Delta b)^2} \quad (1)$$

Color difference can be measured between blank and test samples, as well as at different test points on the same sample. The color difference at different points of the test sample was measured to see if the microcapsules were evenly distributed. If the distribution of microcapsules is uneven and there is aggregation, it will affect the color difference. The L_1 and L_2 represent the brightness values of two different test positions on the same sample. The a_1 and a_2 represent the red and green values of two different test positions on the same sample. The b_1 and b_2 represent the yellow and blue values of two different test positions on the same sample.

According to the GB/T 4893.6-2013 [39], the coating glossiness was tested. The glossiness values of coating at incidence angles of 20°, 60°, and 85° were tested, using a 3nhYG60S glossmeter (Shenzhen San'enshi Technology Co., Ltd., Shenzhen, China).

2.3.4. Mechanical Properties

According to the GB/T 4893.4-2013 [40], coating adhesion was tested using the QFH-A film adhesion tester (Tianjin Yonglida Laboratory Equipment Co., Ltd., Tianjin, China).

According to the GB/T 6739-2006 [41], coating hardness was tested using an HT-6510P pencil hardness tester (Guangzhou Lantai Instrument Co., Ltd., Guangzhou, China). The 9B-9H pencils were selected, in sequence, to push down at least 7 mm on the sample surface, at a speed of approximately 0.5 mm/s. Then, the damage on the surface of the

coatings was observed. When the coating surface is just undamaged, the pencil hardness is the maximum hardness of the coatings.

In accordance with the GB/T 4893.9-1992 [42], coating impact was tested using a QCJ-40 coatings impactor (Shanghai Meiyu Instrument Technology Co., Ltd., Shanghai, China). The maximum height is the maximum impact strength when there is no cracking or peeling of the coating.

Three identical samples were prepared for each type of coating. A universal mechanical testing machine (Changchun Xinte Testing Machine Co., Ltd., Changchun, China) was used to conduct mechanical tensile tests on coatings (original coatings, scratched coatings, and coatings after 1 day of repair). The fracture elongation of coatings was calculated in each state, according to Formula (2). The repair rate of the paint film was represented by the fracture elongation. Formula (3) was used to calculate the repair rate of the coatings [43].

$$E = \frac{L_h - L_0}{L_0} \times 100\% \quad (2)$$

E is the fracture elongation of the coating, L_h is the length between the markings after the coating is broken and assembled, and L_0 is the original length between the markings of the coating.

$$\eta = \frac{E_H - E_S}{E_I - E_S} \times 100\% \quad (3)$$

η is the repair rate of the coating (unit is percentage). E_H is the fracture elongation of the coating after 1 day of repair, E_S is the fracture elongation of the coating after scratches, and E_I is the fracture elongation of the original coating.

2.3.5. Roughness

Before testing, a cloth was used to wipe the coating surface clean, and the test piece was placed on the experimental bench. Ra represents the arithmetic average roughness, which is used to evaluate the overall unevenness of the surface. The Ra value is the average roughness of the coating.

2.3.6. Cold-Liquid Resistance

In accordance with the GB/T 4893.1-2005 [44], an evaluation standard for the cold-liquid resistance level of coatings is shown in Table 7. The color difference and glossiness were tested, concurrently.

Table 7. Evaluation standard for cold-liquid-resistance level of coatings.

| Cold-Liquid Resistance (Level) | Standard |
|--------------------------------|--|
| 1 | The coating has not been damaged. |
| 2 | When illuminated with a light source, a slight discoloration can be observed. |
| 3 | There are slight imprints on the surface. |
| 4 | The imprints are serious, while the structural appearance of the coating has not changed. |
| 5 | The imprints are more serious, and the material structure has been changed, such as blistering, cracking, etc. |

2.3.7. Analysis of Electromagnetic-Absorption Performance

An agilent E8363C vector network analyzer (Agilent Technology (China) Co., Ltd., Beijing, China) was used to measure the electromagnetic-absorption parameters of the blending of three types of microcapsules. The transmission line theory was used to calculate the theoretical reflection loss of the sample. The absorption performance of the material was inversely proportional to the theoretical reflection-loss value.

All the above tests were repeated four times, with an error of less than 5.0%.

3. Results and Discussion

3.1. Analysis of Orthogonal Experimental Results for the Blending of Three Types of Microcapsules

Based on the orthogonal experimental results of the fracture elongation of coatings, the biggest influencing factor on the performance of the coating has been explored. From Table 8, it can be seen that when the content of shellac microcapsules was 3.0%, the content of CIP microcapsules was 1.0%, the content of CIP/CNT microcapsules was 5.0%, and the coating thickness was 20 μm , the highest fracture elongation of the coating was 25.4%. From the variance results of the fracture elongation of coating (Table 8) and the effect curve of the coating fracture elongation (Figure 2), the most critical influencing ingredient was the content of CIP/CNT microcapsules. The content of shellac microcapsules was the second influencing factor. The influence of coating thickness and the content of CIP microcapsules was relatively small, and the impact of the four factors was not significant. Therefore, based on the above results, the CIP microcapsule content was controlled at 1.0%, the primer coating thickness was 10 μm , and the content of the CIP/CNT microcapsules and shellac microcapsules were selected as variables for important-factor experimental analysis.

Table 8. Range and variance results of fracture elongation of coatings.

| Item | Content of Shellac Microcapsules (%) | Content of CIP Microcapsules (%) | Content of CIP/CNT Microcapsules (%) | Primer Coating Thickness (μm) | Fracture Elongation (%) |
|-------------------|--------------------------------------|----------------------------------|--------------------------------------|--|-------------------------|
| 1 # | 1.0 | 1.0 | 1.0 | 10.0 | 11.2 |
| 2 # | 1.0 | 3.0 | 3.0 | 20.0 | 13.7 |
| 3 # | 1.0 | 5.0 | 5.0 | 25.0 | 16.4 |
| 4 # | 2.0 | 1.0 | 3.0 | 25.0 | 18.3 |
| 5 # | 2.0 | 3.0 | 5.0 | 10.0 | 23.7 |
| 6 # | 2.0 | 5.0 | 1.0 | 20.0 | 12.9 |
| 7 # | 3.0 | 1.0 | 5.0 | 20.0 | 25.4 |
| 8 # | 3.0 | 3.0 | 1.0 | 25.0 | 14.5 |
| 9 # | 3.0 | 5.0 | 3.0 | 10.0 | 20.6 |
| Mean 1 | 13.767 | 18.300 | 12.867 | 18.500 | - |
| Mean 2 | 18.300 | 17.300 | 17.533 | 17.333 | - |
| Mean 3 | 20.167 | 16.633 | 21.833 | 16.400 | - |
| R | 6.400 | 1.667 | 8.966 | 2.100 | - |
| DEVSQ | 64.996 | 4.222 | 120.669 | 6.642 | - |
| degree of freedom | 2.000 | 2.000 | 2.000 | 2.000 | - |
| F ratio | 1.323 | 0.086 | 2.456 | 0.135 | - |
| F critical value | 4.460 | 4.460 | 4.460 | 4.460 | - |
| Significance | - | - | - | - | - |

3.2. Effect of Blending of Three Types of Microcapsules on the Optical Properties

From Table 9, with the fixed content of shellac microcapsules, the color difference in the coating gradually increased with the increase of CIP/CNT microcapsule content. With the fixed shellac microcapsules of 2.0%, when the content of CIP/CNTs microcapsules was 9.0%, the largest color difference in the coating was 2.78. When the content of CIP/CNT microcapsules increased from 4.0% to 9.0%, the color-difference change in the coating was 1.57. This is because the three types of microcapsules have different particle sizes, resulting in uneven dispersion in the coating. Moreover, when using the SZQ four-sided coating preparation device to apply coatings, larger microcapsules may be hindered by the coating preparation device, and this might generate accumulation. The higher the content of microcapsules, the poorer the dispersion and the more obvious the accumulation. Therefore, there is a greater change in color difference [45].

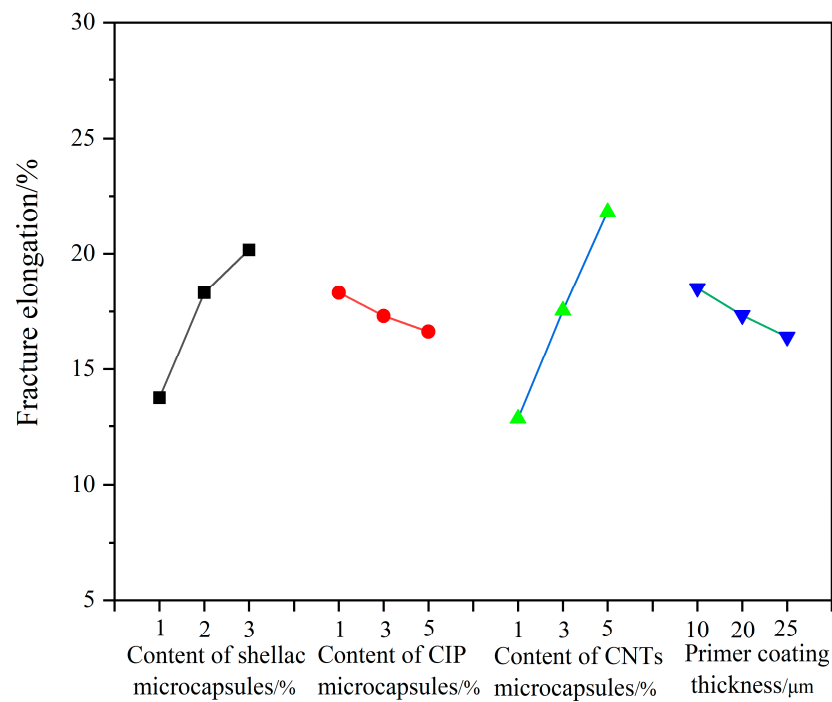


Figure 2. Effect curve of fracture elongation of coating.

Table 9. The effect of blending of three types of microcapsules on the color value and color difference of coatings.

| Content of Shellac Microcapsules (%) | Content of CIP/CNT Microcapsules (%) | L_1 | a_1 | b_1 | L_2 | a_2 | b_2 | ΔL | Δa | Δb | ΔE |
|--------------------------------------|--------------------------------------|-------|-------|-------|-------|-------|-------|------------|------------|------------|------------|
| Blank | 0 | 48.63 | 11.49 | 25.32 | 48.65 | 11.19 | 25.6 | -0.02 | 0.30 | -0.28 | 0.41 |
| 2.0 | 4.0 | 42.74 | 10.82 | 18.39 | 42.66 | 10.43 | 17.95 | 0.08 | 0.39 | 0.44 | 0.59 |
| | 5.0 | 40.58 | 8.34 | 17.39 | 41.25 | 9.16 | 16.63 | -0.67 | -0.82 | 0.76 | 1.30 |
| | 6.0 | 37.15 | 6.88 | 16.18 | 35.84 | 7.70 | 16.55 | 1.31 | -0.82 | -0.37 | 1.59 |
| | 7.0 | 35.19 | 5.75 | 13.70 | 36.76 | 5.77 | 13.06 | -1.57 | -0.02 | 0.64 | 1.70 |
| | 8.0 | 33.51 | 4.31 | 10.60 | 31.50 | 3.74 | 11.50 | 2.01 | 0.57 | -0.90 | 2.27 |
| | 9.0 | 28.39 | 4.28 | 9.72 | 25.87 | 5.34 | 10.25 | 2.52 | -1.06 | -0.53 | 2.78 |
| 4.0 | 4.0 | 43.29 | 11.24 | 20.35 | 43.86 | 11.59 | 20.13 | -0.57 | -0.35 | 0.22 | 0.70 |
| | 5.0 | 41.56 | 10.58 | 19.36 | 42.32 | 10.98 | 19.82 | -0.76 | -0.40 | -0.46 | 0.97 |
| | 6.0 | 39.86 | 9.25 | 17.68 | 38.99 | 9.83 | 16.82 | 0.87 | -0.58 | 0.86 | 1.35 |
| | 7.0 | 32.45 | 6.02 | 15.76 | 33.63 | 6.54 | 14.26 | -1.18 | -0.52 | 1.50 | 1.98 |
| | 8.0 | 30.46 | 5.74 | 13.45 | 29.83 | 6.12 | 11.56 | 0.63 | -0.38 | 1.89 | 2.03 |
| | 9.0 | 29.58 | 4.56 | 11.34 | 30.84 | 5.82 | 9.94 | -1.26 | -1.26 | 1.40 | 2.27 |

From Table 10, it can be seen that the glossiness of coatings with 2.0% and 4.0% shellac microcapsules showed varying degrees of decrease with the increased CIP/CNT microcapsules. When the content of CIP/CNT microcapsules was constant, the glossiness trend of coatings with different shellac microcapsule contents was basically consistent. This indicated that the content of shellac microcapsules had less impact on the coating glossiness. On the one hand, the content of shellac microcapsules accounts for a relatively small proportion in the blending of the three types of microcapsules, which has little effect on the glossiness of the coating. On the other hand, the shellac microcapsules are light-yellow solid powders, while CIP microcapsules and CIP/CNT microcapsules are grayish-black in color. When the content of CIP/CNTs microcapsules is higher, it can mask the color development of shellac microcapsules. When the content of shellac microcapsules and CIP/CNTs microcapsules was 4.0% and 9.0%, respectively, the minimum glossiness of the coating was 19.6 GU at 60 ° glossiness. Compared with the lowest glossiness value

of 11.2 GU in the article by Wu et al. [37], the negative impact of the blending of the three types of microcapsules on the glossiness of the coating was smaller.

Table 10. The effect of blending of three types of microcapsules on the coating glossiness.

| Content of Shellac Microcapsules (%) | Content of CIP/CNT Microcapsules (%) | 20° Glossiness (GU) | 60° Glossiness (GU) | 85° Glossiness (GU) |
|--------------------------------------|--------------------------------------|---------------------|---------------------|---------------------|
| Blank | 0 | 17.5 | 42.1 | 47.4 |
| 2.0 | 4.0 | 14.1 | 38.6 | 40.8 |
| | 5.0 | 10.8 | 34.7 | 36.5 |
| | 6.0 | 7.3 | 32.3 | 29.4 |
| | 7.0 | 5.4 | 26.5 | 27.3 |
| | 8.0 | 4.8 | 24.3 | 25.6 |
| | 9.0 | 3.5 | 21.6 | 20.7 |
| 4.0 | 4.0 | 13.6 | 36.7 | 39.4 |
| | 5.0 | 11.5 | 33.4 | 35.2 |
| | 6.0 | 9.4 | 31.2 | 27.6 |
| | 7.0 | 5.2 | 25.4 | 25.4 |
| | 8.0 | 3.9 | 22.1 | 20.8 |
| | 9.0 | 3.1 | 19.6 | 17.6 |

3.3. Effect of Blending of Three Types of Microcapsules on the Mechanical Properties and Roughness

From Table 11, the effects of blending three types of microcapsules on the mechanical properties and roughness of the coating can be seen. The adhesion level of the coating was directly proportional to the content of microcapsules, with a maximum of level 3. It can be seen that the mixed-microcapsule powder has no effect on the adhesion ability of the coating. The hardness of the coating is proportional to the content of microcapsules. When the content of shellac microcapsules and CIP/CNTs microcapsules was 4.0% and 7.0%, respectively, the maximum hardness reached 5H, and the impact strength reached a maximum of 21 kg·cm. This is because different types of microcapsule particles have different strengths and enhancement effects on the impact resistance of the coating. The dispersion and uniformity of microcapsules in the coating also have an effect on the impact resistance of the coating [46]. On the basis of Table 11, the blending of three types of microcapsules improved the impact strength of the coating. The roughness of the coating gradually ascended with the increase in the content of the blending of three types of microcapsules. The coating with a 4.0% content of shellac microcapsules had a higher overall roughness. This is because the overall content of blending microcapsules is high, which makes them less likely to disperse in the coating.

3.4. Effect of Blending of Three Types of Microcapsules on the Fracture Elongation and Repair Rate

The tensile test results of the coating with the blending of three types of microcapsules are shown in Table 12. When the content of microcapsules was 0–7%, the fracture elongation of the coating added with microcapsules shows an upward trend. When the microcapsule content was 7–9%, the fracture elongation decreased (Figure 3). The overall fracture elongation of the coating with 4.0% content of shellac microcapsules was higher than that of the coating with 2.0% content of shellac microcapsules. This is because shellac has good viscosity. The increase in the content of shellac microcapsules indicates that there is more shellac in the coating, thus enhancing the tensile resistance of the coating. When the content of shellac microcapsules was 4.0% and the content of CIP/CNTs microcapsules was 7.0%, the fracture elongation and repair rate of the coating were the highest, reaching 20.1% and 33.9%, respectively. This is because when three different microcapsules act on the coating at the same time, each different core material microcapsule has different periods of action and ability to withstand external forces when the coating is strained to varying degrees.

The method of mixed addition has matching microcapsules to withstand external forces of different periods. Therefore, the fracture elongation of the coating has been improved.

Table 11. The effect of blending of three types of microcapsules on the mechanical properties and roughness of coatings.

| Content of Shellac Microcapsules (%) | Content of CIP/CNT Microcapsules (%) | Adhesion (Grade) | Hardness | Impact Resistance (kg·cm) | Ra (μm) |
|--------------------------------------|--------------------------------------|------------------|----------|---------------------------|---------|
| Blank | 0 | 1 | H | 8 | 0.516 |
| 2.0 | 4.0 | 1 | 2H | 9 | 0.543 |
| | 5.0 | 1 | 2H | 10 | 0.919 |
| | 6.0 | 2 | 3H | 12 | 1.546 |
| | 7.0 | 2 | 3H | 15 | 1.694 |
| | 8.0 | 2 | 3H | 18 | 1.891 |
| | 9.0 | 3 | 4H | 14 | 2.092 |
| 4.0 | 4.0 | 1 | 2H | 10 | 0.919 |
| | 5.0 | 1 | 2H | 13 | 1.069 |
| | 6.0 | 1 | 3H | 17 | 1.502 |
| | 7.0 | 2 | 4H | 21 | 1.728 |
| | 8.0 | 2 | 4H | 15 | 1.905 |
| | 9.0 | 2 | 5H | 12 | 2.239 |

Table 12. The effect of blending of three types of microcapsules on the fracture elongation and self-healing performance.

| Content of Shellac Microcapsules (%) | Content of CIP/CNT Microcapsules (%) | Fracture Elongation (%) | | | Repair Rate (%) |
|--------------------------------------|--------------------------------------|-------------------------|------------------|-----------------|-----------------|
| | | Original | After Scratching | After Repairing | |
| Blank | 0 | 5.3 | 3.8 | 3.1 | |
| 2.0 | 4.0 | 10.3 | 6.9 | 7.5 | 17.6 |
| | 5.0 | 12.5 | 9.0 | 9.7 | 20.0 |
| | 6.0 | 14.2 | 10.5 | 11.3 | 21.6 |
| | 7.0 | 16.8 | 11.1 | 12.5 | 24.6 |
| | 8.0 | 15.7 | 10.5 | 11.5 | 19.2 |
| | 9.0 | 13.5 | 9.7 | 10.4 | 18.4 |
| 4.0 | 4.0 | 11.4 | 7.6 | 8.3 | 18.4 |
| | 5.0 | 13.9 | 9.8 | 10.7 | 22.0 |
| | 6.0 | 16.7 | 11.7 | 13.1 | 28.0 |
| | 7.0 | 20.1 | 14.5 | 16.4 | 33.9 |
| | 8.0 | 17.4 | 12.1 | 13.3 | 22.6 |
| | 9.0 | 15.2 | 11.8 | 12.5 | 20.5 |

Shellac microcapsules have good self-healing performance. When the coating is stimulated by external forces or temperature changes to produce cracks, the shellac microcapsules at the crack tip rupture, due to concentrated stress. The repair agent of shellac flows out and seeps into the crack, under capillary action. The repair agent undergoes a cross-linking polymerization reaction, causing crack closure.

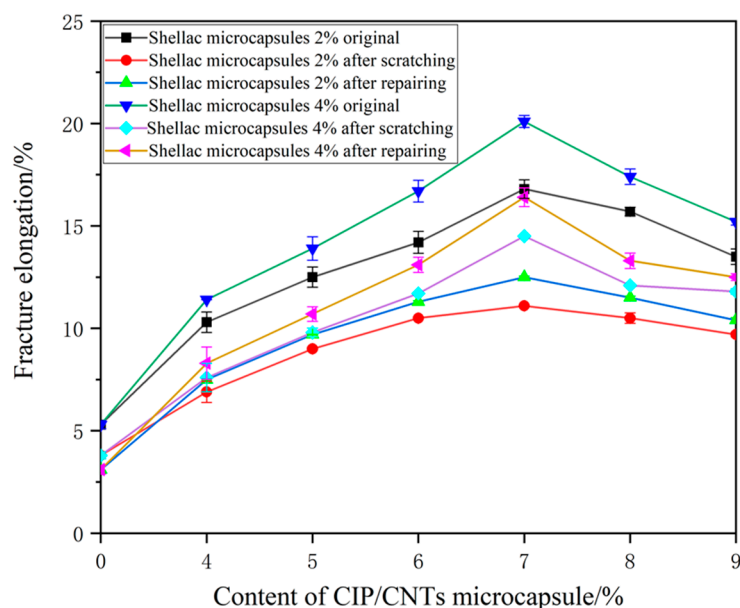


Figure 3. The influence curves of different microcapsule contents on the fracture elongation of the original coating, after scratching and after repairing.

3.5. Effect of Blending of Three Types of Microcapsules on the Microscopic Morphology

The coating exhibited better comprehensive performance when the content of shellac microcapsules was 4.0%, the content of CIP microcapsules was 1.0%, and the content of CIP/CNT microcapsules was 7.0%. Figure 4 shows SEM morphology of the coating with 4.0% shellac microcapsules, 1.0% CIP microcapsule content, and 6.0%, 7.0%, and 8.0% CIP/CNT microcapsule content, respectively. As the content of CIP/CNT microcapsules increased, uneven spots gradually appeared in the coating. Because the microcapsules have a certain volume and shape, the presence of microcapsules will occupy the pores in the coating. This leads to increased interfacial friction between coating matrix and microcapsules. Moreover, high-content microcapsules are more prone to particle aggregation, which affects the dispersion of microcapsules in the coating and makes the coating smoother [47].

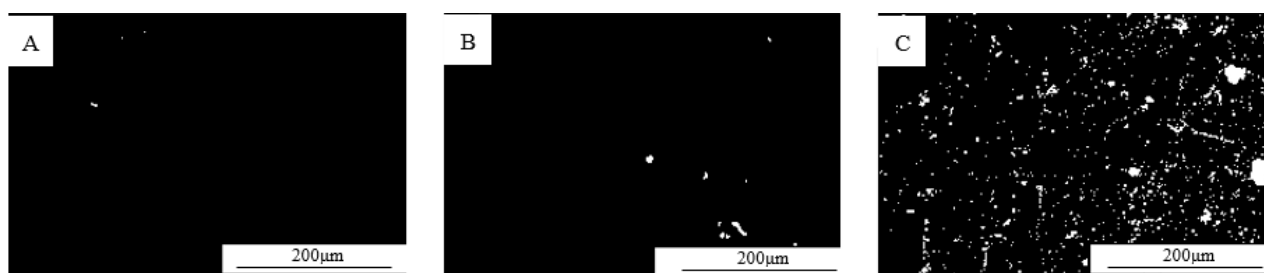


Figure 4. SEM morphology of the coating added with different CIP/CNT microcapsule contents: (A) 6.0%, (B) 7.0%, and (C) 8.0%, respectively.

3.6. Infrared Analysis of Blending of Three Types of Microcapsules

Figure 5 is the infrared spectra of coatings with content of 4.0% shellac microcapsules and 6.0%, 7.0%, and 8.0% CIP/CNT microcapsules, respectively. The broad and strong peak appearing at 3357 cm^{-1} was the N-H stretching vibration absorption peak. The absorption peak at 2865 cm^{-1} belonged to the stretching vibration peak of $-\text{CH}_2$. The peak at 1725 cm^{-1} was the C=O stretching vibration peak of polyester [48]. The absorption peak at 1521 cm^{-1} belonged to the $-\text{NH}-$ stretching vibration peak. The absorption peak at 1350 cm^{-1} was the bending vibration peak of $-\text{CN}$, and the bending vibration absorption peak of the triazine ring in melamine resin appeared at 813 cm^{-1} .

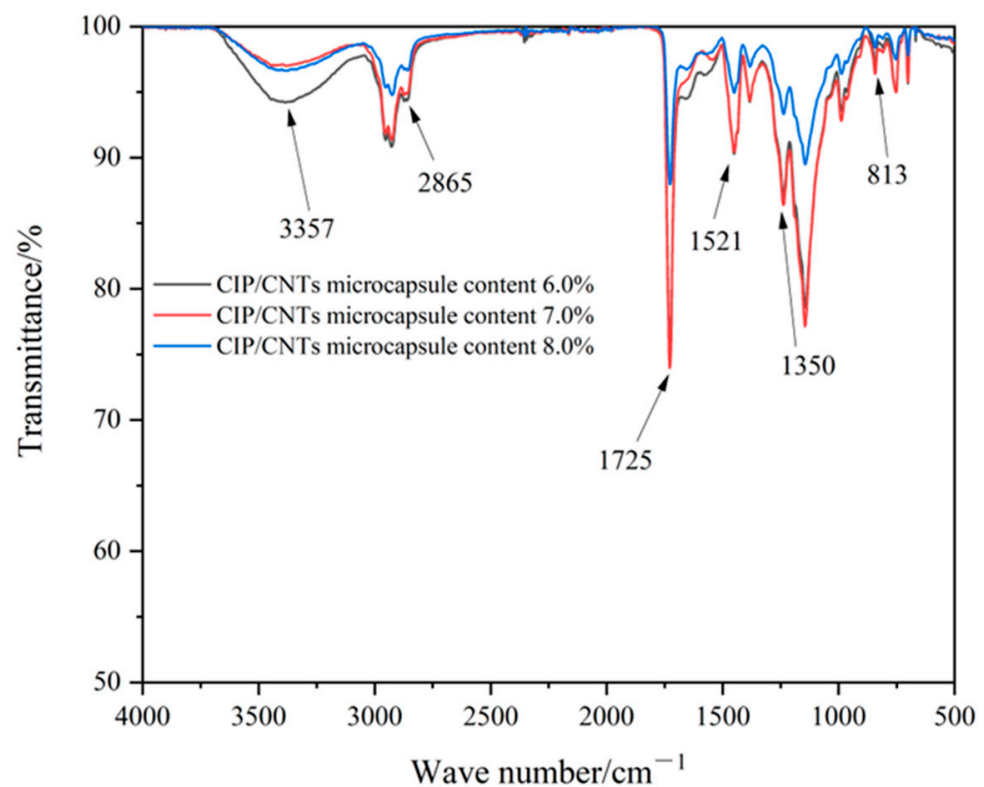


Figure 5. Infrared spectrum of coatings with different CIP/CNT microcapsule contents.

When irradiated with infrared light, chemical bonds or functional groups in the molecule can undergo vibration (or rotation) absorption. Different chemical bonds or functional groups have different absorption frequencies, and are located at different positions on the infrared spectrum. This indicates information on what chemical bonds or functional groups are present in the molecule. The information on chemical bonds or functional groups remains unchanged, indicating that there is no reaction between the microcapsules and the coating. Figure 5 demonstrates that microcapsules do not react or dissolve in water-based coatings, and exist independently. The electromagnetic-absorption performance and self-healing properties of microcapsules can also enable coatings to achieve these two properties.

3.7. Effect of Blending of Three Types of Microcapsules on the Cold-Liquid Resistance

Table 13 shows the cold-liquid-resistance levels of coatings prepared by the blending of three types of microcapsules in different contents. Figures 6–9 show the changes in color difference and glossiness values of coatings after resistance to four different liquids. The color difference in the red-ink coating after resistance to cold liquid changed significantly, with a level 5, while the impact of the other three cold liquids was relatively small, with levels of 1 and 2. Because the red ink contains solvent that can cause damage to the coating, such as alcohol and ether solvents, the coating dissolves and is dispersed in the solvent. Due to the uneven color marks left by red ink on the surface of the coating, the range of the color-difference change was relatively large. The fluctuation in color difference in coatings with 2.0% content of shellac microcapsules was smaller, compared to coatings with 4.0% content of shellac microcapsules. The glossiness of coatings prepared by the blending of three types of microcapsules showed a decreasing trend at a 60° incidence angle, with a gradual and uniform decrease.

Table 13. Cold-liquid-resistance level of coatings prepared by blending of the three types of microcapsules.

| Content of Shellac Microcapsules (%) | Content of CIP/CNT Microcapsules (%) | Cold-Liquid-Resistance Level (Level) | | | |
|--------------------------------------|--------------------------------------|--------------------------------------|------------------|--------------------------|--|
| | | 75.0% Ethanol Solution | Red Ink Solution | 70.0% Detergent Solution | 15.0% Sodium Chloride Aqueous Solution |
| Blank | 0 | 2 | 5 | 1 | 2 |
| 2.0 | 4.0 | 1 | 5 | 1 | 1 |
| | 5.0 | 1 | 5 | 1 | 1 |
| | 6.0 | 2 | 5 | 1 | 1 |
| | 7.0 | 1 | 5 | 1 | 1 |
| | 8.0 | 1 | 5 | 1 | 1 |
| | 9.0 | 1 | 5 | 1 | 1 |
| 4.0 | 4.0 | 1 | 5 | 1 | 1 |
| | 5.0 | 1 | 5 | 1 | 2 |
| | 6.0 | 1 | 5 | 1 | 2 |
| | 7.0 | 1 | 5 | 1 | 1 |
| | 8.0 | 1 | 5 | 1 | 1 |
| | 9.0 | 2 | 5 | 1 | 1 |

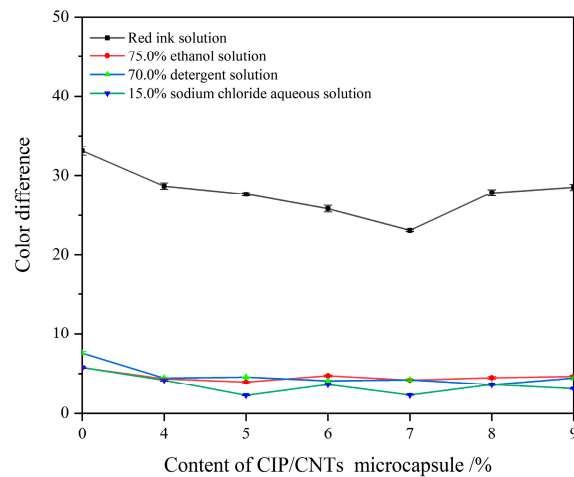


Figure 6. Effect of CIP/CNTs microcapsules on the color difference after cold-liquid resistance with the shellac microcapsules of 2.0%.

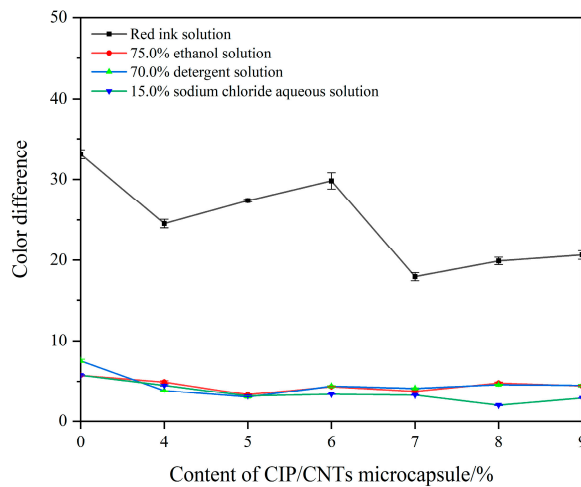


Figure 7. Effect of CIP/CNT microcapsules on the color difference after cold-liquid resistance with the shellac microcapsules of 4.0%.

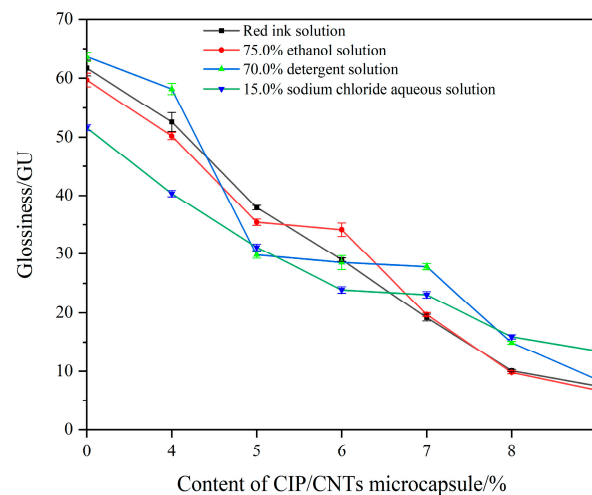


Figure 8. Effect of CIP/CNT microcapsules on the glossiness after cold-liquid resistance with the shellac microcapsules of 2.0%.

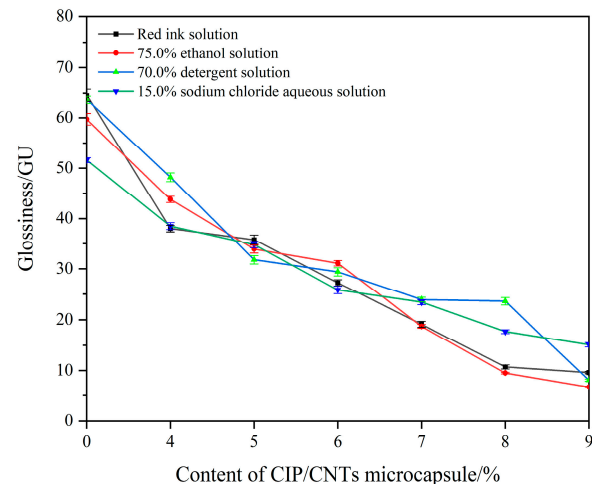


Figure 9. Effect of CIP/CNT microcapsules on the glossiness after cold-liquid resistance with the shellac microcapsules of 4.0%.

3.8. Electromagnetic-Absorption Performance of Blending of Three Types of Microcapsules

The previous test results showed that the overall performance of the coating was better when 4.0% shellac microcapsules, 1.0% CIP microcapsules, and 7.0% CIP/CNTs microcapsules were added. At this point, the content of shellac microcapsules was 33.3%, the content of CIP microcapsules was 8.4%, and the content of CIP/CNT microcapsules was 58.3%. This mixed-microcapsule powder was analyzed for electromagnetic-absorption performance, and the electromagnetic-absorption effect was investigated. Figures 10–12 show the dielectric constant, magnetic permeability, and theoretical reflection loss of the blending of three types of microcapsules, respectively. When the matching thickness was 3.5 mm, the mixed-microcapsule powder exhibited two effective absorption bands, namely 4.3 GHz–8.1 GHz and 13.9 GHz–17.8 GHz, respectively. The theoretical minimum reflection loss of -14.28 dB was obtained at 17.6 GHz. Compared with the previous result (Table 14), the blending of three types of microcapsules improved the electromagnetic-absorption performance, while ensuring the optical and mechanical properties of the coating. This is because the blending of shellac microcapsules, CIP microcapsules, and CIP/CNT microcapsules can change the transmission path of electromagnetic waves, increasing the absorption of the electromagnetic wave and exhibiting a good electromagnetic-absorption performance at relatively wide frequencies. By blending microcapsules, the electromagnetic-

absorption characteristics of various microcapsules can be fully utilized to improve the frequency-response range of the powder [49].

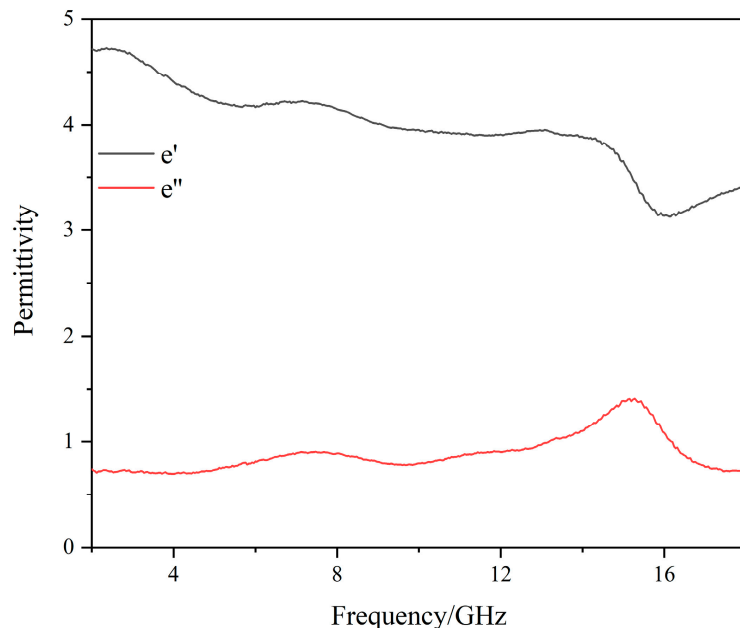


Figure 10. Dielectric constants of blending of shellac, CIP, and CIP/CNT microcapsules.

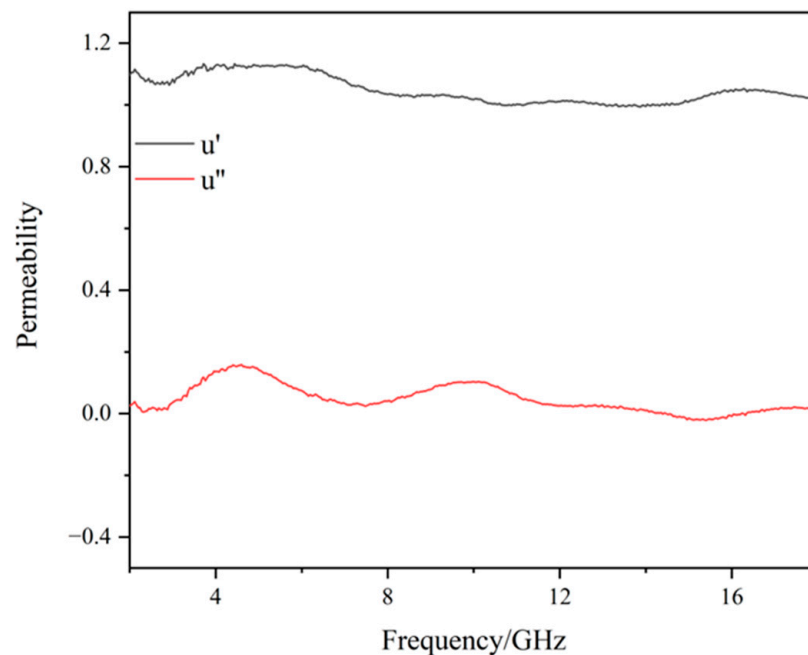


Figure 11. Magnetic permeability of blending of shellac, CIP, and CIP/CNT microcapsules.

Table 14. Comparison table of electromagnetic-absorption properties.

| Sample | Frequency Band < -5 dB | Minimum Reflection Loss |
|-----------------|---------------------------------------|-------------------------|
| Xia et al. [35] | 8.2 GHz–17 GHz | -7.94 dB at 11.8 GHz |
| Li et al. [36] | 15.3 GHz–16.2 GHz | -6.53 dB at 15.8 GHz |
| Wu et al. [37] | 15.3 GHz–18 GHz | -13.52 dB at 16.2 GHz |
| Current sample | 4.3 GHz–8.1 GHz and 13.9 GHz–17.8 GHz | -14.28 dB at 17.6 GHz |

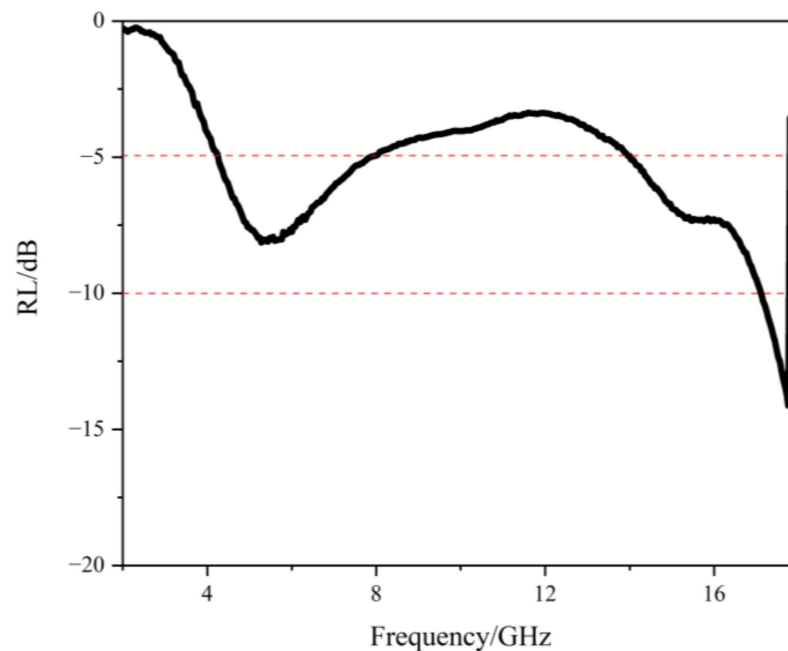


Figure 12. Theoretical reflection loss of blending of shellac, CIP, and CIP/CNTs microcapsules.

4. Conclusions

The biggest factor affecting the tensile properties of the coating was the content of CIP/CNT microcapsules, followed by the content of shellac microcapsules. The content of CIP microcapsules and the thickness of the primer coating had little effect on the tensile properties of the coating. When the content of shellac microcapsules was 4.0% and the content of CIP/CNTs microcapsules was 7.0%, the color difference in the coating was 1.98, the glossiness was 25.4 GU, the adhesion was level 2, the hardness reached 4H, the impact strength was 21 kg·cm, and the roughness was 1.728 μm . The fracture elongation of the coating reached 20.1%, with the best self-healing performance, and a repair rate of 33.9%. The addition of mixed-microcapsule powder did not change the chemical structure of the coating. The coating had the poor cold-liquid resistance to red-ink solution, but good cold-liquid resistance to 75.0% ethanol solution, 70.0% detergent solution, and 15.0% sodium chloride aqueous solution. When the content of shellac microcapsules was 33.3%, the content of CIP microcapsules was 8.4%, and the content of CIP/CNT microcapsules was 58.3%, the mixed-microcapsule powder showed two effective absorption bands, 4.3 GHz–8.1 GHz and 13.9 GHz–17.8 GHz, respectively. The theoretical minimum reflection loss of -14.28 dB was achieved at 17.6 GHz. The results effectively expanded the absorption-frequency band, and enhanced the electromagnetic-absorption performance, which provides a new approach for application of the self-healing and electromagnetic-absorption dual-functional water-based coatings.

Author Contributions: Conceptualization and methodology, Y.Z.; writing—review and editing, W.L.; validation, resources, Y.X.; data management, J.H.; formal analysis, investigation, X.Y.; supervision, J.L. All authors have read and agreed to the published version of the manuscript.

Funding: This project was partly supported by the Natural Science Foundation of Jiangsu Province (BK20201386).

Institutional Review Board Statement: Not applicable.

Informed Consent Statement: Not applicable.

Data Availability Statement: Data are contained within the article.

Conflicts of Interest: The authors declare that there are no conflicts of interest.

References

1. Panzarasa, G.; Burgert, I. Designing functional wood materials for novel engineering applications. *Holzforschung* **2022**, *76*, 211–222. [[CrossRef](#)]
2. Zhou, C.; Huang, T.; Luo, X.; Kaner, J. Reorganisation and construction of an age-friendly smart recreational home system: Based on function–capability match methodology. *Appl. Sci.* **2023**, *13*, 9783. [[CrossRef](#)]
3. Hu, W.; Liu, N.; Xu, L.; Guan, H. Study on cold/warm sensation of materials used in desktop of furniture. *Wood Res.-Slovakia* **2020**, *65*, 497–506. [[CrossRef](#)]
4. Luo, Y.R.; Xu, W. Optimization of panel furniture plates rework based on intelligent manufacturing. *Bioresources* **2023**, *18*, 5198–5208. [[CrossRef](#)]
5. Luo, Z.Y.; Xu, W.; Wu, S.S. Performances of green velvet material (PLON) used in upholstered furniture. *Bioresources* **2023**, *18*, 5108–5119. [[CrossRef](#)]
6. Weng, M.Y.; Zhu, Y.T.; Mao, W.G.; Zhou, J.C.; Xu, W. Nano-silica/urea-formaldehyde resin-modified fast-growing lumber performance study. *Forests* **2023**, *14*, 1440. [[CrossRef](#)]
7. Chen, Y.T.; Sun, C.S.; Ren, Z.R.; Na, B. Review of the current state of application of wood defect recognition technology. *BioResources* **2023**, *18*, 2288–2302. [[CrossRef](#)]
8. Hu, W.; Luo, M.; Liu, Y.; Xu, W.; Konukcu, A.C. Experimental and numerical studies on the mechanical properties and behaviors of a novel wood dowel reinforced dovetail joint. *Eng. Fail. Anal.* **2023**, *152*, 107440. [[CrossRef](#)]
9. Danilov, V.; Ayzenshtadt, A.; Kilyusheva, N.; Belyaev, A. Wood surface modification with an arabinogalactan–silica composition. *J. Wood Chem. Technol.* **2021**, *41*, 269–281. [[CrossRef](#)]
10. Li, R.; Yao, Q.; Wang, X. Optimization of cutting power and power efficiency during particleboard helical milling. *Materialwiss. Werkstofftech.* **2023**, *54*, 158–167. [[CrossRef](#)]
11. Hu, W.; Wan, H. Comparative study on weathering durability properties of phenol formaldehyde resin modified sweetgum and southern pine specimens. *Maderas-Cienc. Tecnol.* **2022**, *24*, 17. [[CrossRef](#)]
12. Wang, C.; Zhang, C.Y.; Ding, K.Q.; Jiang, M.H. Immersion polishing post-treatment of PLA 3D printed formed parts on its surface and mechanical performance. *BioResources* **2023**, *18*, 7995–8006. [[CrossRef](#)]
13. Wang, C.; Zhou, Z. Optical properties and lampshade design applications of PLA 3D printing materials. *BioResources* **2023**, *18*, 1545–1553. [[CrossRef](#)]
14. Ling, K.L.; Feng, Q.M.; Huang, Y.H.; Li, F.; Huang, Q.F.; Zhang, W.; Wang, X.C. Effect of modified acrylic water-based paint on the properties of paint film. *Spectrosc. Spect. Anal.* **2020**, *40*, 2133–2137.
15. Li, R.; He, C.; Xu, W.; Wang, X.A. Prediction of surface roughness of CO₂ laser modified poplar wood via response surface methodology. *Maderas-Cienc. Tecnol.* **2022**, *24*, 1–12. [[CrossRef](#)]
16. Zhang, X.; Wang, P.F.; Sun, D.W.; Li, X.; An, J.L.; Yu, T.X.; Yang, E.H.; Yang, J.L. Dynamic plastic deformation and failure mechanisms of individual microcapsule and its polymeric composites. *J. Mech. Phys. Solids* **2020**, *139*, 103933. [[CrossRef](#)]
17. Arenas-Jal, M.; Suñé-Negre, J.M.; García-Montoya, E. An overview of microencapsulation in the food industry: Opportunities, challenges, and innovations. *Eur. Food Res. Technol.* **2020**, *246*, 1371–1382. [[CrossRef](#)]
18. Morsy, M.K.; Elsabagh, R. Quality parameters and oxidative stability of functional beef burgers fortified with microencapsulated cod liver oil. *LWT-Food Sci. Technol.* **2021**, *142*, 110959. [[CrossRef](#)]
19. Sardroud, H.A.; Nemati, S.; Khoshfetrat, A.B.; Nabavinia, M.; Khosrowshahi, Y.B. Barium-cross-linked alginate-gelatine microcapsule as a potential platform for stem cell production and modular tissue formation. *J. Microencapsul.* **2017**, *34*, 488–497. [[CrossRef](#)]
20. Lee, M.W.; An, S.; Yoon, S.S.; Yarin, A.L. Advances in self-healing materials based on vascular networks with mechanical self-repair characteristics. *Adv. Colloid Interface Sci.* **2018**, *252*, 21–37. [[CrossRef](#)]
21. White, S.R.; Sottos, N.R.; Geubelle, P.H.; Moore, J.S.; Kessler, M.R.; Sriram, S.; Brown, E.N.; Viswanathan, S. Autonomic healing of polymer composites. *Nature* **2001**, *409*, 794–797. [[CrossRef](#)] [[PubMed](#)]
22. Kessler, M.R.; Sottos, N.R.; White, S.R. Self-healing structural composite materials. *Compos. Part A* **2003**, *34*, 743–753. [[CrossRef](#)]
23. Suryanarayana, C.; Rao, K.C.; Kumar, D. Preparation and characterization of microcapsules containing linseed oil and its use in self-healing coatings. *Prog. Org. Coat.* **2008**, *63*, 72–78. [[CrossRef](#)]
24. Si, W.; Liao, Q.W.; Hou, W.; Chen, L.Y.; Li, X.L.; Zhang, Z.W.; Sun, M.N.; Song, Y.J.; Qin, L. Low-frequency broadband absorbing coatings based on MOFs: Design, fabrication, microstructure and properties. *Coatings* **2022**, *12*, 766. [[CrossRef](#)]
25. Chen, J.B.; Zheng, J.; Huang, Q.Q.; Wang, F.; Ji, G.B. Enhanced microwave absorbing ability of carbon fibers with embedded FeCo/CoFe₂O₄ nanoparticles. *ACS Appl. Mater. Interfaces* **2021**, *13*, 36182–36189. [[CrossRef](#)]
26. Hu, Y.J.; Zhao, H.J.; Yu, X.D.; Li, J.W.; Zhang, B.; Li, T.T. Research progress of magnetic field regulated mechanical property of solid metal materials. *Metals* **2022**, *12*, 1988. [[CrossRef](#)]
27. Yan, H.H.; Song, X.H.; Wang, Y. Study on wave absorption properties of carbonyl iron and SiO₂ coated carbonyl iron particles. *AIP Adv.* **2018**, *8*, 065322. [[CrossRef](#)]
28. Lokhat, D.; Carsky, M. Direct coal liquefaction using iron carbonyl powder catalyst. *Chem. Eng. Technol.* **2019**, *42*, 818–826. [[CrossRef](#)]

29. Shen, J.B.; Wang, B.; Cai, L.W.; Liu, L.D.; Zhang, C.; Wang, B.X.; Tian, Y.; Yu, Y.D.; Dong, J.Q.; Wang, G.D. Magnetic properties and thermal stability of Fe-based amorphous/carbonyl iron soft magnetic composites. *J. Mater. Sci. Mater. Electron.* **2023**, *34*, 1169. [[CrossRef](#)]
30. Ni, J.L.; Hu, F.; Feng, S.J.; Kan, X.C.; Han, Y.Y.; Liu, X.S. Soft magnetic properties of FeSiAl/carbonyl iron composites with high magnetic permeability and low magnetic loss. *J. Alloys Compd.* **2021**, *887*, 161337. [[CrossRef](#)]
31. Kochetkov, K.A.; Vasil'eva, T.T.; Gasanov, R.G.; Mysova, N.E.; Bystrova, N.A. The use of iron carbonyls in the C-C bond formation reactions. *Russ. Chem. Bull.* **2019**, *28*, 1301–1320. [[CrossRef](#)]
32. Liu, J.Q.; Dong, Y.N.; Wang, P.; Zhu, Z.Q.; Pang, J.; Li, X.Y.; Zhang, J.Q. Improved high-frequency magnetic properties of FeSiBCCr amorphous soft magnetic composites by adding carbonyl iron powders. *J. Non-Cryst. Solids* **2023**, *605*, 122166. [[CrossRef](#)]
33. Zheng, Z.R.; Li, S.G.; Peng, K. Magnetic properties regulation and loss contribution analysis of FeSi soft magnetic composites doped by carbonyl iron powders. *J. Magn. Magn. Mater.* **2023**, *568*, 170423. [[CrossRef](#)]
34. Gong, M.J.; Dong, Y.Q.; Huang, J.J.; Chang, L.; Pan, Y.; Wang, F.L.; He, A.N.; Li, J.W.; Liu, X.C.; Wang, X.M. The enhanced magnetic properties of FeSiCr powder cores composited with carbonyl iron powder. *J. Mater. Sci. Mater. Electron.* **2021**, *32*, 8829–8836. [[CrossRef](#)]
35. Xia, Y.X.; Li, W.B.; Yan, X.X. Effect of shellac microcapsules blended with carbonyl iron powder and carbon nanotubes on the self-healing and electromagnetic wave absorption properties of waterborne coatings on fiberboard surface. *Coatings* **2023**, *13*, 1572. [[CrossRef](#)]
36. Li, W.B.; Yan, X.X. Effects of shellac self-repairing and carbonyl iron powder microcapsules on the properties of Dulux waterborne coatings on wood. *Polymers* **2023**, *15*, 2016. [[CrossRef](#)] [[PubMed](#)]
37. Wu, Q.L.; Li, W.B.; Yan, X.X. Effect of microcapsules on mechanical, optical, self-healing and electromagnetic wave absorption in waterborne wood paint coatings. *Coatings* **2023**, *13*, 1478. [[CrossRef](#)]
38. GB/T 11186.3-1989; Methods for Measuring the Color of Coatings—Part 3: Calculation of Color Difference. Standardization Administration of the People's Republic of China: Beijing, China, 1989.
39. GB/T 4893.6-2013; Testing of Physical and Chemical Properties of Furniture Surface Paint Films—Part 6: Gloss Determination Method. Standardization Administration of the People's Republic of China: Beijing, China, 2013.
40. GB/T 4893.4-2013; Testing of Physical and Chemical Properties of Furniture Surface Paint Films—Part 4: Determination of Adhesion Cross Cut Method. Standardization Administration of the People's Republic of China: Beijing, China, 2013.
41. GB/T 6739-2006; Paints and Varnishes—Determination of Film Hardness by Pencil Test. Standardization Administration of the People's Republic of China: Beijing, China, 2006.
42. GB/T 4893.9-2013; Test of Surface Coatings of Furniture—Part 9: Determination of Resistance to Impact. Standardization Administration of the People's Republic of China: Beijing, China, 2013.
43. GB/T 4893.1-2021; Test of Surface Coatings of Furniture—Part 1: Determination of Surface Resistance to Cold Liquids. Standardization Administration of the People's Republic of China: Beijing, China, 2021.
44. Han, Y.; Yan, X.X.; Tao, Y. Effect of transparent, purple, and yellow shellac microcapsules on the optical properties and self-healing performance of waterborne coatings. *Coatings* **2022**, *12*, 1056. [[CrossRef](#)]
45. Sun, Y.X.; Zhang, X.W.; Zhao, D.Y. Reinforcement of aminopropyl-terminated siloxane-treated carbon nanotubes in epoxy thermosets: Mechanical and thermal properties. *Polymers* **2023**, *15*, 3184. [[CrossRef](#)]
46. Hong, M.K.; Choi, W.K.; Park, J.H.; Kuk, Y.S.; Kim, B.S.; Seo, M.K. Relationship between functionalized multi-walled carbon nanotubes and damping properties of multi-walled carbon nanotubes/carbon fiber-reinforced plastic composites for shaft. *J. Nanosci. Nanotechnol.* **2020**, *20*, 6862–6870. [[CrossRef](#)]
47. Zhang, M.Y.; Lu, J.X.; Li, P.; Li, X.J.; Yuan, G.M.; Zuo, Y.F. Construction of high-efficiency fixing structure of waterborne paint on silicate-modified poplar surfaces by bridging with silane coupling agents. *Prog. Org. Coat.* **2022**, *167*, 106846. [[CrossRef](#)]
48. Bociaga, D.; Sobczyk-Guzenda, A.; Szymanski, W.; Jedrzejczak, A.; Jastrzebska, A.; Olejnik, A.; Swiatek, L.; Jastrzebski, K. Diamond like carbon coatings doped by Si fabricated by a multi-target DC-RF magnetron sputtering method—Mechanical properties, chemical analysis and biological evaluation. *Vacuum* **2017**, *143*, 395–406. [[CrossRef](#)]
49. Munir, A. Microwave radar absorbing properties of multiwalled carbon nanotubes polymer composites: A review. *Adv. Polym. Technol.* **2017**, *36*, 21617. [[CrossRef](#)]

Disclaimer/Publisher's Note: The statements, opinions and data contained in all publications are solely those of the individual author(s) and contributor(s) and not of MDPI and/or the editor(s). MDPI and/or the editor(s) disclaim responsibility for any injury to people or property resulting from any ideas, methods, instructions or products referred to in the content.